

## University of Groningen

### New Features of the Morphotropic Phase Boundary in the Pb(Zr<sub>1-x</sub>Ti<sub>x</sub>)O<sub>3</sub> System

Nohedá, B.; Gonzalo, J.A.; Caballero, A.C.; Moure, C.; Cox, D.E.; Shirane, G.

*Published in:*  
Ferroelectrics

*DOI:*  
[10.1080/00150190008216254](https://doi.org/10.1080/00150190008216254)

**IMPORTANT NOTE:** You are advised to consult the publisher's version (publisher's PDF) if you wish to cite from it. Please check the document version below.

*Document Version*  
Publisher's PDF, also known as Version of record

*Publication date:*  
2000

[Link to publication in University of Groningen/UMCG research database](#)

*Citation for published version (APA):*  
Nohedá, B., Gonzalo, J. A., Caballero, A. C., Moure, C., Cox, D. E., & Shirane, G. (2000). New Features of the Morphotropic Phase Boundary in the Pb(Zr<sub>1-x</sub>Ti<sub>x</sub>)O<sub>3</sub> System. *Ferroelectrics*, 237(1), 237/[54-1]-244/[548]. <https://doi.org/10.1080/00150190008216254>

**Copyright**  
Other than for strictly personal use, it is not permitted to download or to forward/distribute the text or part of it without the consent of the author(s) and/or copyright holder(s), unless the work is under an open content license (like Creative Commons).

The publication may also be distributed here under the terms of Article 25fa of the Dutch Copyright Act, indicated by the "Taverne" license. More information can be found on the University of Groningen website: <https://www.rug.nl/library/open-access/self-archiving-pure/taverne-amendment>.

**Take-down policy**  
If you believe that this document breaches copyright please contact us providing details, and we will remove access to the work immediately and investigate your claim.

*Downloaded from the University of Groningen/UMCG research database (Pure): <http://www.rug.nl/research/portal>. For technical reasons the number of authors shown on this cover page is limited to 10 maximum.*

## New Features of the Morphotropic Phase Boundary in the $\text{Pb}(\text{Zr}_{1-x}\text{Ti}_x)\text{O}_3$ System

B. NOHEDA<sup>a</sup>, J. A. GONZALO<sup>a</sup>, A.C. CABALLERO<sup>b</sup>, C. MOURÉ<sup>b</sup>,  
 D.E. COX<sup>c</sup> and G. SHIRANE<sup>c</sup>

<sup>a</sup>*Universidad Autonoma de Madrid, Cantoblanco, 28049-Madrid, Spain*, <sup>b</sup>*Instituto de Ceramica y Vidrio, CSIC, Arganda, 28500-Madrid, Spain* and <sup>c</sup>*Brookhaven National Laboratory, Upton, NY 11973-5000, USA*

(Received July 12, 1999)

Recently a new monoclinic phase in the  $\text{Pb}(\text{Zr}_{1-x}\text{Ti}_x)\text{O}_3$  ceramic system has been reported by Noheda et al.<sup>[1]</sup> for a composition of  $x=0.48$ . In this work, samples with Ti contents  $x=0.47$  and 0.50, which are both tetragonal below their Curie point, have been investigated. In the sample with  $x=0.50$ , the tetragonal phase was found to transform to a monoclinic phase at about 200 K as the temperature was lowered. The sample with  $x=0.47$  showed a complicated region of phase coexistence between ~ 440K-320K, becoming rhombohedral at around 300 K. No further symmetry change was found down to 20K. Dielectric measurements for these two samples are also reported. On the basis of these results, a preliminary phase diagram is presented. Optimum compositional homogeneity is needed to properly characterize the new monoclinic region.

**Keywords:** Ferroelectrics; PZT; Structure; Perovskite; Monoclinic phase; Morphotropic phase boundary

### INTRODUCTION

The basic features of the  $\text{Pb}(\text{Zr}_{1-x}\text{Ti}_x)\text{O}_3$  (PZT) phase diagram were determined in the 1950's<sup>[2]</sup>. The ceramic PZT system has the cubic perovskite  $\text{ABO}_3$  structure at high temperatures. On lowering the temperature the materials undergo a phase transition to a ferroelectric phase for all compositions except those close to pure  $\text{PbZrO}_3$ , where they become antiferroelectric. The ferroelectric region is divided in two phases with

different symmetries by a morphotropic phase boundary (MPB), nearly vertical in temperature, occurring at a composition close to  $x \approx 0.47$ . The Ti-rich region has tetragonal symmetry ( $F_r$ , space group  $P4mm$ ) and the Zr-rich region has rhombohedral symmetry ( $F_r$ ). The latter is divided into high-temperature ( $F_{RHT}$ , space group  $R3c$ ) and low-temperature ( $F_{RLT}$ , space group  $R3m$ ) zones respectively.<sup>4,5,9</sup>

Most of the studies on PZT have been performed for compositions around the MPB motivated both by the interesting physical properties and the technologically-useful applications, such as high electromechanical coupling factors and permittivities, exhibited by PZT at this boundary<sup>9,10</sup>. Due to compositional fluctuations, the MPB often appears as an ill-defined region of phase coexistence, instead of a well defined boundary, whose size depends of the processing conditions<sup>17,9</sup>. This fact has for many years hindered a detailed interpretation of the nature of the  $F_r$ - $F_r$  phase transition and the MPB itself. In order to explore the MPB in more detail, we have embarked upon a systematic structural study using high-resolution synchrotron x-ray powder diffraction techniques and dielectric measurements to characterize the samples.

A recent unexpected result obtained from high-resolution x-ray measurements on a sample of high compositional homogeneity with  $x \approx 0.48$ , was the discovery of a ferroelectric phase with monoclinic symmetry below approximately 250K<sup>11</sup>. The monoclinic unit cell is such that  $a_m$  and  $b_m$  lie along the tetragonal  $[1\ 1\ 0]$  and  $[1\ 1\ 0]$  directions ( $a_m \approx b_m \approx a\sqrt{2}$ ), and  $c_m$  is close to the  $[001]$  axis ( $c_m \approx c$ ). The temperature dependence of the monoclinic angle  $\beta$ , the angle between  $a_m$  and  $c_m$  gives the evolution of the order parameter for the tetragonal-monoclinic ( $F_r$ - $F_m$ ) phase transition. Two other compositions prepared under slightly different conditions with  $x \approx 0.47$  and  $x \approx 0.50$  were also studied at that time, and in the present paper we report results for these materials and propose a preliminary modification of the PZT phase diagram around the MPB.

## EXPERIMENTAL

Two different compositions of PZT with Ti contents of 0.47 and 0.50 were prepared by a solid-state reaction from  $PbO_2$ ,  $ZrO_2$  and Nb-free  $TiO_2$  with chemical purities better than 99.9%. The mixed powders were calcined at 790°C, remilled, isostatically pressed at 200 Mpa, and sintered at 1200°C for 2h, with heating and cooling rates of 3°C/min. To minimize the volatilization of lead oxide, alumina crucibles with tightly-fitting covers were used and a mixture of  $PbZrO_3$ +5% wt  $ZrO_2$  was used as a lead source in the crucible. The densities measured by the liquid displacement method were  $\geq 98\%$  of the theoretical values.

High-resolution synchrotron x-ray powder diffraction measurements were made at beam line X7A at the Brookhaven National Synchrotron Light Source. A Ge(111) double-crystal monochromator was used in combination with a Ge(220) analyser, with wavelengths of 0.6896 Å for  $x = 0.47$  and 0.7995 Å for  $x = 0.50$ . In this configuration, the instrumental resolution,  $\Delta 2\theta$ , is slightly better than 0.01° in the  $2\theta$  region 0-30°, an order-of-magnitude better than that of a conventional laboratory instrument. The pellets were mounted in symmetric reflection geometry and scans were made over selected peaks in the low-angle region of the pattern. Since lead is a strong absorber, the penetration depth below the surface of the pellet at  $2\theta = 20^\circ$  is only about 2  $\mu\text{m}$ . Measurements were made at various temperatures between 20-790 K for  $x = 0.47$  and from 20-300 K, for  $x = 0.50$ . Measurements above room temperature were performed with the pellet mounted on a flat BN sample holder inside a wire-wound BN tube furnace. The accuracy of the temperature was estimated to be within 5 K, and the temperature stability was  $\sim 2$  K. For measurements below room temperature, the sample was mounted on a flat Cu sample holder in a closed-cycle He cryostat. In this case, the estimated accuracy of the temperature was 1K, with a stability of  $\sim 0.1$  K. The angular regions scanned were chosen so as to cover the pseudo-cubic (100), (110), (111), (200), (220) and (222) reflections, with a  $2\theta$  step interval of 0.005 or 0.01° depending on the peak widths. Dielectric measurements were performed with a precision LCR meter (Hewlett Packard-4284A) increasing temperature at a constant rate of 0.5 K/min. and with a temperature accuracy better than 0.1 K.

## RESULTS AND DISCUSSION

Based on the analysis of the diffraction data for the PZT compositions studied in this work ( $x = 0.47$  and 0.50) and that previously reported for  $x = 0.48^{(1)}$ , we propose a modification of the PZT phase diagram<sup>(6)</sup> around its MPB, which include the new monoclinic phase as shown in Fig. 1, where temperatures below 300K are also shown. As can be seen, the MPB in Jaffe's phase diagram corresponds to the phase boundary between the  $F_r$  and the  $F_m$  phases, but the  $F_r$ - $F_m$  phase boundary is still not well defined.

Fig. 2 shows that the monoclinic phase is found to exist for  $x = 0.50$  below room temperature. From peak fits based on a pseudo-Voigt peak function, at 20 K the (111)<sub>c</sub> pseudo-cubic reflection is found to consist of three different peaks corresponding to the monoclinic (201), (021) and (201) reflections while the pseudo-cubic (220)<sub>c</sub> is split into four peaks corresponding to the (222), (222), (400) and (040) monoclinic reflections. The last two are fairly close to each other, indicating that the difference between  $a_m$  and  $b_m$  is quite small. As the temperature increases the monoclinic

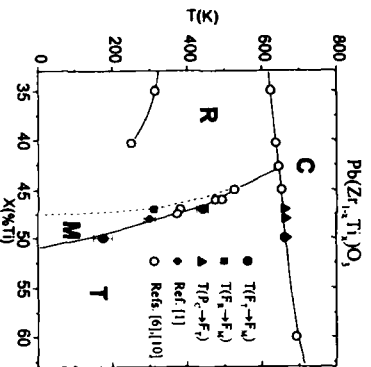


FIGURE 1 Preliminary modification of the PZT phase diagram around its MPB obtained from the results of this work. Data in refs.[6](p.136) and [10]( $x=0.40$ ) are plotted as open circles. Data of  $x=0.48$ <sup>[1]</sup> are also included.

splitting becomes less evident. For  $T=150\text{K}$ , (400) and (040), at  $2\theta \approx 32.62^\circ$  cannot be resolved, showing that  $a_m \approx b_m$ . For  $T > 200\text{K}$ , the monoclinic features, if any, cannot be detected, and the observed reflections can be indexed on the basis of a tetragonal unit cell. The evolution of the lattice parameters for temperatures below  $300\text{K}$  is shown in Fig. 3.

The PZT composition with  $x=0.47$  was found to be rhombohedral from  $20\text{-}300\text{K}$ . Fig. 4 shows the temperature evolution of the (111)<sub>r</sub> and (200)<sub>r</sub> pseudo-cubic reflections between  $300\text{-}787\text{K}$ . At  $300\text{K}$  (111)<sub>r</sub> is split into rhombohedral (111) and (111) peaks, while (200)<sub>r</sub> remains a single peak, corresponding to rhombohedral (220). For  $300\text{K} < T < 440\text{K}$  there is a region where the peak profiles broaden in a complex way suggesting the gradual evolution of a second phase which is difficult to characterize (see  $T=372$  and  $425\text{K}$  in Fig. 4). This could simply reflect the coexistence of rhombohedral and tetragonal phases accompanied by a considerable amount of internal strain, but it is certainly not possible to rule out the formation of small regions of the monoclinic phase. For  $T$  above  $\sim 450\text{K}$ , the tetragonal phase can be clearly identified although there is still some residual diffuse scattering in the vicinity of rhombohedral (200). Finally, at  $T \approx 665\text{K}$ , the cubic phase appears. The temperature evolution of the lattice parameters is shown in Fig. 5. We note that the peak profiles in the cubic region are about twice as broad as those found for the  $x \approx 0.48$  sample<sup>[1]</sup>, indicative of a smaller crystallite size and wider range of compositional inhomogeneity. This is probably associated with the slightly different sintering temperatures used for the preparation of the samples,  $1200$  and  $1250^\circ\text{C}$  respectively.

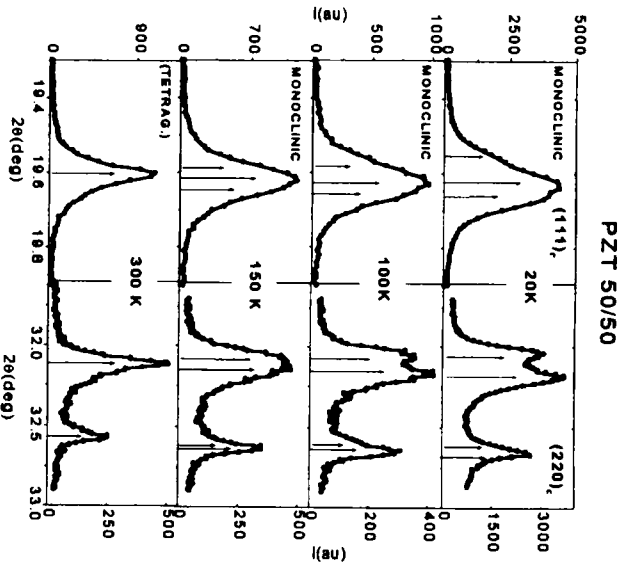


FIGURE 2 (111)<sub>c</sub> and (220)<sub>c</sub> pseudo-cubic reflections at different temperatures for  $\text{PbZr}_{0.50}\text{Ti}_{0.50}\text{O}_3$ .

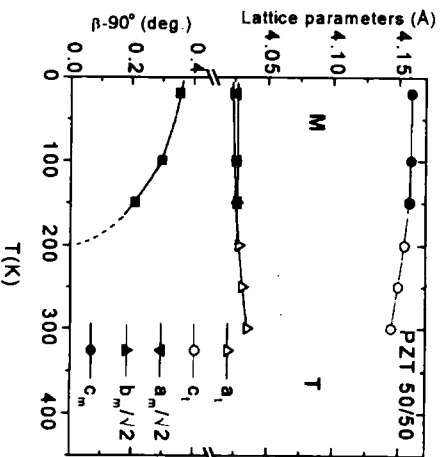


FIGURE 3 Lattice parameters vs.  $T$  for  $x = 0.50$  in the monoclinic ( $a_m$ ,  $b_m$ ,  $c_m$ ,  $\beta$ ) and tetragonal ( $a_t$ ,  $c_t$ ) phases.

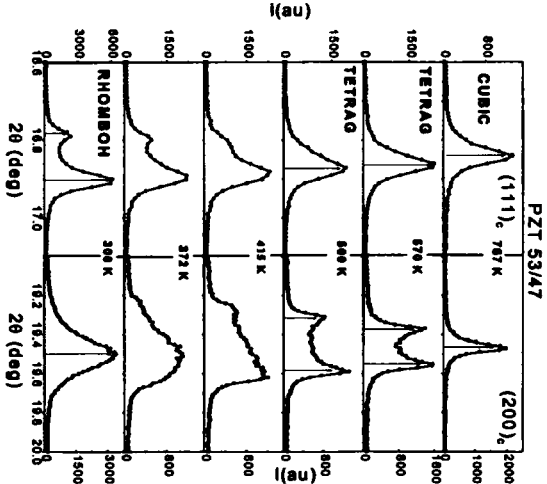


FIGURE 4 (111)<sub>c</sub> and (200)<sub>t</sub> pseudo-cubic reflections at different temperatures for PbZr<sub>0.53</sub>Ti<sub>0.47</sub>O<sub>3</sub>. Note the improved resolution compared to the laboratory x-ray data reported by Mishra *et al.* [12]

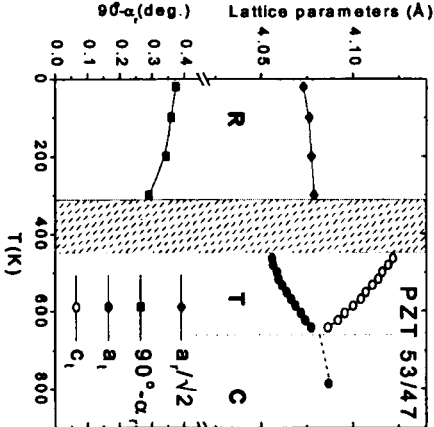


FIGURE 5 Lattice parameters vs. T for x=0.47 in the rhombohedral (a<sub>r</sub>, α<sub>r</sub>) and tetragonal (a<sub>t</sub>, c<sub>t</sub>) phases. The complex region of phases coexistence is shown shaded in the plot.

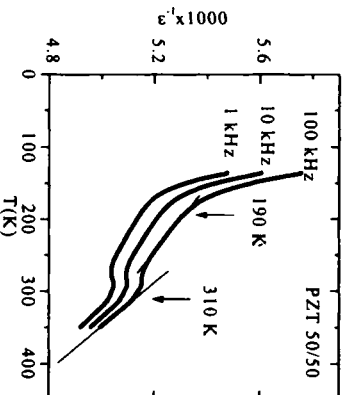


FIGURE 6. Inverse of the dielectric permittivity vs. temperature for three different frequencies for  $\text{PbZr}_{0.50}\text{Ti}_{0.50}\text{O}_3$ .

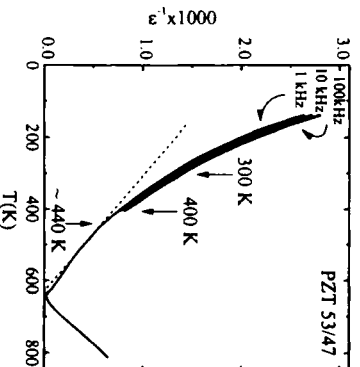


FIGURE 7. Inverse of the dielectric permittivity vs. temperature for three different frequencies for  $\text{PbZr}_{0.51}\text{Ti}_{0.49}\text{O}_3$ . At  $T > 400$  K only data at 1 kHz are shown for clarity. Note the change of slope at  $\sim 440$  K shown by the broken lines, and the two arrows at 300 and 400 K, which correspond to the region of thermal hysteresis reported by Zhang et al.<sup>[11]</sup>

The dielectric permittivity,  $\epsilon$ , was measured along the axis of the pellets at 1, 10 and 100 kHz for both compositions as the temperature was raised from 140 K.  $\epsilon^{-1}$  is plotted in Fig. 6 for  $x = 0.50$  in the interval 140 K <  $T < 350$  K. Two changes of slope are clearly observed as temperature values decrease, the first one at  $\sim 310$  K, and the second at  $\sim 190$  K. It is possible that the first of these two anomalies could correspond to the onset of a local



monoclinic distortion even though we were unable to resolve any monoclinic splitting ( $a_m=b_m$ ). The anomaly at  $T \approx 190$  K would then correspond to the onset of the long-range distortion below which  $a_m \neq b_m$ .

The inverse of the dielectric permittivity with increasing temperature is plotted in Fig. 7 for  $x = 0.47$ . In the region below the cubic-tetragonal transition at 640 K, there is an increase in slope in the region around 440 K as indicated by the broken lines, while at lower temperatures the slope continues to increase, but without any sharp discontinuities indicative of a well-defined transition. The results are generally consistent with the diffraction evidence for phase coexistence and the possible existence of a monoclinic phase. The permittivity data are in good agreement with those recently reported by Zhang *et al.*<sup>[11]</sup>, who also found thermal hysteresis effects between 300–400 K which they interpreted as the coexistence of rhombohedral and tetragonal phases. A R-T coexistence region between 473–533 K was also inferred by Mishra *et al.*<sup>[12]</sup> for a sample with  $x=0.535$  on the basis of planar coupling coefficient measurements and laboratory x-ray data.

This work clearly demonstrates the need for both excellent compositional homogeneity and high instrumental resolution for the determination of the features of the PZT phase diagram around the MPB. Further work along these lines is in progress.

#### ACKNOWLEDGMENTS

We thank L.E. Cross and R. Guo for their stimulating discussions. Support by NATO (R.C.G. 970037), Spanish CICYT (PB96-0037) and U.S. Department of Energy (contract No. DE-AC 02-98 CH10886) is also acknowledged.

#### References

- [1] B. Noheda, D.E. Cox, G. Shirane, J. Gonzalo, E. Park, L.E. Cross, *Appl. Phys. Lett.* **74**(14), 2059 (1999). <<http://xxx.lanl.gov/abs/cond-mat/9903007>>.
- [2] G. Shirane, K. Suzuki, *J. Phys. Soc. Japan* **7**, 333 (1952). E. Sawaguchi, *J. Phys. Soc. Japan* **8**, 615 (1953).
- [3] H. Barnett, *J. Appl. Phys.* **33**, 1606 (1962).
- [4] C. Michel, J. Moreau, G. Achenbach, R. Gerson, W. James, *Solid State Com.* **7**, 865 (1969).
- [5] A. M. Glazer and S. A. Mabud, *Acta Cryst* **B34**, 1060 (1978).
- [6] B. Jaffe, W. Cook, and H. Jaffe, *Piezoelectric Ceramics* (Acad. London, 1971).
- [7] P. Art-Gur, L. Benguigui, *Sol. Stat. Comm.* **15**, 1077 (1974).
- [8] K. Kakewaga, O. Matsunaga, T. Kato and Y. Sasaki, *J. Am. Ceram. Soc.* **78**(41), 1071 (1995).
- [9] J. Fernandes, D. Hall, M. Cockburn and G. Greaves, *Nucl. Instr. and Meth. In Phys. Res.* **B97**, 137 (1995).
- [10] A. Amin, R. Newnham, E. Cross, D. Cox, *J. Solid State Chem.* **37**, 248 (1981).
- [11] S. Zhang, X. Dong, S. Kojima, *Jpn. J. Appl. Phys.* **36**, 2994–2997 (1997).
- [12] S. K. Mishra, D. Pandey, *Appl. Phys. Lett.* **69**, 1707–1709 (1996).